Proceedings World Geothermal Congress 2026
Calgary, Canada, June 8 – 11, 2026

Shock Cooling Assisted Drilling: Thermo-Mechanical Coupled Modeling of Rock Weakening and MSE Reduction

E. Jahangir[2], B. Goelema[1]*, L. Gerbaud[2], A. Rogers[1], A. Vetsak[1]
Eavor Technologies Inc. Calgary AB, Canada[1],
Mines Paris - PSL research university, geosciences département, Fontainebleau, France[2]
bart.goelema@eavor.com

Keywords: shock cooling, homogeneous granite, thermo-mechanical FEM, high-temperature, cooling fluid

ABSTRACT

This work explores the feasibility of the shock cooling (defined as the rapid quenching of hot rock by cold fluid) effect on the mechanical specific energy during cutting, both experimentally and numerically. First a single cutter test was performed on Red Bohus granite sample, and a Polycrystalline Diamond Compact cutter was used at laboratory scale under different high temperatures and cooling modes. Then a fully coupled thermo-mechanical finite element model was developed using the Abaqus software under a dynamic explicit framework to simulate the interaction between the cutter and granite in the presence of a cooling fluid. The fluid–structure interaction around cutters under controlled cooling scenarios was handled by an explicit (Coupled Eulerian/Lagrangian) method. The simulation setup includes dynamic heat transfer, thermal front propagation, and damage-based element deletion to capture progressive rock removal. The work highlights the importance of thermal propagation relative to cutter engagement. Specifically, the model captures when thermal front propagation becomes less beneficial at high rates of penetration in drilling, if the thermal front depth is significantly shallower than the cutting depth. This study provides a numerical framework for assessing thermally assisted drilling concepts, with potential applications in improving the efficiency and durability of geothermal well construction operations.

1 INTRODUCTION

Deep geothermal energy is increasingly recognized as a sustainable solution for global energy needs. With recent advancements in high-temperature drilling and subsurface reservoir characterization, exploiting deeper and hotter crystalline basement, predominantly represented by granitic formations, has become more technically feasible (Khodayar and Bjornsson, 2024). However, the drilling cost of deeper geothermal wells can become unbearable due to long tripping times to replace a worn-out drill bit after experiencing early damage of the bit when drilling a granitic formation. To reduce the price per geothermal energy unit for end users, the bit life should be extended, and the rate of penetration should be increased. Wear of the PDC bit faces can be reduced by making the drilling process smoother. One possible solution could be the weakening process by quenching rock with cold water in a concept known as shock (rapid) cooling while drilling. Modeling the hot granitic rock interacting with cooler drilling fluid within fractions of seconds during the drilling process, introduces significant challenges. Numerous studies have aimed to quantify and model how thermal stress, especially under rapid cooling (quenching), affects granite's integrity and consequently ability to smoothen the drilling process with Polycrystalline Diamond Compact (PDC) bits.

The objective of this study is to evaluate the potential advantages of the shock cooling process through both numerical simulations and experimental study in the context of granitic formation drilling.

The literature review on cooling processes of thermally treated granite samples shows that the majority of research-based investigations have focused on samples that have been subjected to an initial heating phase reaching a predetermined target temperature, followed by a cooling phase, the rate of which varies (Shen et al, 2021). During this cooling phase, various mechanical and physical properties of the rock are systematically monitored. Within the temperature range of 100-300 °C, the heating phase does not significantly affect the mechanical properties. In contrast, the cooling phase exerts a substantial influence, dependent upon its cooling rate and method. Beyond 300 °C, high temperature granite shows all mechanical indicator degradation (P-wave UCS: Uniaxial Compressive Strength and UTS: Uniaxial Tensile Strength and Young's modulus) followed by a much higher degradation during the cooling phase (Zhang et al., 2021; Shen et al., 2021). In this study, we focus on rock formations with an initial temperature ranging from 150 °C to 200 °C and then will undergo a cooling phase. It is hypothesized that the heating phase does not significantly alter the mechanical properties of the

rocks, whereas the cooling phase is expected to have a substantial weakening impact on the rock. This imposed thermal stress path should correspond to the drilling phase, that will be explored both experimentally and numerically.

The reduction in macroscopic strength of granite subjected to elevated temperatures is primarily governed by progressive weakening of interfacial transition zones, rather than intrinsic mineral degradation (Ma et al., 2025). For the sake of simplification, this study focuses on macroscopic homogeneous type modeling; a more detailed heterogeneous approach can be found in our recent work (Jahangir et al., 2025).

2 BACKGROUND & METHODOLOGY

Granite is a polymineralic rock composed primarily of quartz, feldspar, and biotite, which possess different thermal expansion coefficients. When subjected to elevated temperatures, differential expansion initiates microcracks, predominantly at grain boundaries. Quenching through water or other liquids, further amplifies damage by inducing steep thermal gradients (Xiao et al., 2021).

Microscopic observations (e.g., SEM imaging) reveal that intergranular cracking dominates early thermal cycling, gradually transitioning to intragranular fracturing at higher cycle counts.

The mechanical deterioration of granite depends strongly on the cooling regime. Air cooling leads to more gradual degradation, while water and liquid nitrogen (LN_2) quenching induce extensive microcracking (Wu et al., 2019).

In order to examine the thermal effect during the drilling process, we devised an experimental setup involving a single PDC cutter. This apparatus facilitates the interaction of the rock specimen with a surrounding fluid medium of varying temperature (Figure 1). Then, an FEA model under dynamic conditions was developed to simulate this experiment considering the applied fluid.

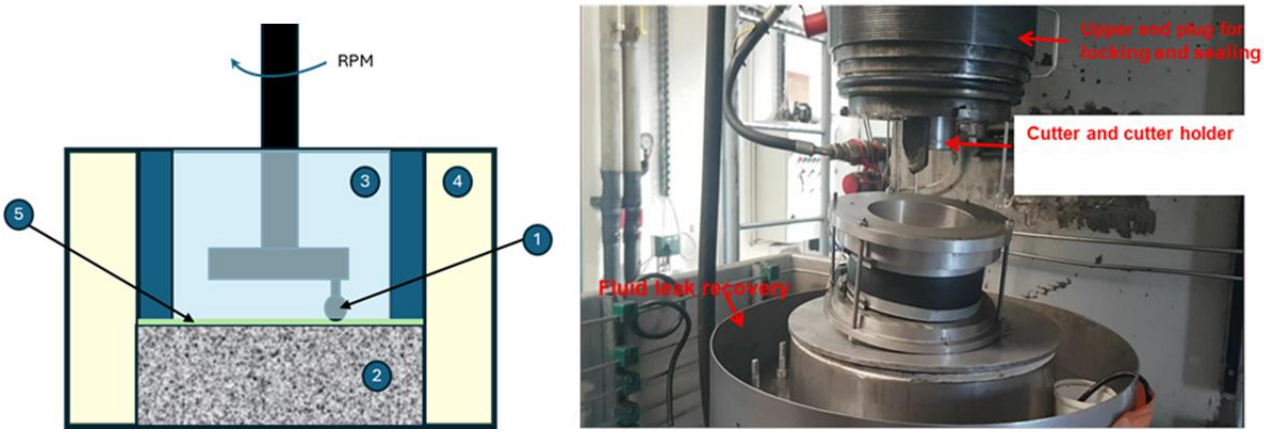


Figure 1. The experimental device: 1) PDC cutter, 2) granite sample, 3) fluid, 4) displacement piston enabling vertical movement of the rock sample, 5) temporary thermal insulation.

2.1 Experimental Setup

Figure 1 illustrates the experimental apparatus, wherein a Red Bohus granite specimen, with a diameter of 14 cm and a thickness of 5 cm, was subjected to cutting. Initially, the sample was heated to a temperature of 200 °C. Subsequently, it was positioned within the apparatus, insulated by a 5-mm-thick polystyrene layer designed to segregate the fluid or air from the heated rock. To ensure the sealing of the cell, the axial displacement (corresponding to the depth of cut or DOC) is applied by the upward movement of the rock sample using the displacement piston. The temporary thermal insulation, originally introduced to ensure the rock sample retains as much heat as possible after the sample leaves the oven, will be removed easily by the PDC cutter. Then, the cutter of 16 mm diameter with a given rake angle (19° herein) can attack the rock sample where the axial load, axial displacement, angular velocity and force are controlled. In this work a DOC of 1 mm and a Rotation per Minute (RPM) of 114 were applied.

2.2 Constitutive Framework for Thermo-Mechanical Damage

To realistically simulate how granite weakens while being cut, we use a well-established model that tracks the rock damage. We adopt a pressure–dependent Drucker–Prager (DP) yield surface for the rock matrix with a scalar damage variable $D \in [0,1]$ that modifies the cohesion and frictional and dilatancy angles (equations 1-3). For the rock undergoing a shearing mechanism, imposed by the cutter, the DP family models are quite relevant (Liu et al., 2019). Equation 1 and 2 show the failure criterion and non-associated plastic potential.

$$f(\sigma, D) = \sqrt{J_2} + \alpha(D) \cdot I_1 - k(D) \leq 0 \quad (1)$$

$$g(\sigma, D) = \sqrt{(J_2)} + \alpha_g(D) \cdot I_1 \quad (2)$$

I_1 and J_2 are the first and second invariants of the stress tensor such as $q = \sqrt{(3J_2)}, p = -I_1/3$. The following equations present the evolution of mechanical parameters where φ is the friction angle, C is the cohesion and ψ is the dilatancy angle.

$$\alpha(D) = \sqrt{(2/9)} \cdot sin(\varphi(D)) \,/\, [3 - sin(\varphi(D))] \quad (3)$$

$$k(D) = 2C \cdot cos(\varphi(D)) \,/\, [3 - sin(\varphi(D))]$$

$$\alpha_g(D) = \sqrt{(2/9)} \cdot sin(\psi(D)) \,/\, [3 - sin(\psi(D))]$$

Plastic strain rate is given by $\dot{\varepsilon}^{\mathrm{p}} = \dot{\lambda}\, \partial \mathrm{g} / \partial \sigma$ where $\dot{\lambda}$ is the plastic multiplier and $\partial \mathrm{g} / \partial \sigma$ gives the plastic flow's direction. The mechanical damage parameter is given by $D_m = \frac{\varepsilon^p}{\varepsilon^p_{max}}$ where ε^p is current plastic strain and ε^p_{max} corresponds to maximum plastic strain at failure.

The evolution of friction and dilatancy angles follow: $\varphi(D) = \varphi_0 \cdot (1 - D), \psi(D) = \psi_0 + \beta D \cdot \psi_0$ where β is dimensionless coefficient controlling the degradation, φ_0 and ψ_0 are respectively intact friction and dilatancy angles.

To capture the degradation of granite under thermal treatment, we adopt a thermoplastic damage parameter inspired by the work of Saksala (2024). Thermal damage D_{t} is evaluated based on the following equation:

$$D_{\mathrm{t}} = \max[1, (K\alpha\Delta T - UTS)/UTS\ ]$$

Where α is the thermal expansion coefficient, ΔT is the temperature difference between the initial temperature and the temperature after cooling., K is the bulk modulus of the granite. The total damage D is defined as the maximum of mechanical and thermal damage components $D = \max[D_{\mathrm{m}}, D_{\mathrm{t}}]$.

This combined damage model effectively integrates both the thermally induced macroscopic damage and mechanically accumulated plastic deformation, offering a realistic framework for simulating granite deterioration under geothermal conditions. The numerical simulation was performed with the finite element software Abaqus (Dassault Systèmes, 2024) where the modified DP model was implemented by a Fortran subroutine. Figure 2 illustrates the calibration phase under triaxial conditions, wherein a Red Bohus granite specimen is exposed to a confining pressure of 20 MPa and ambient temperature and the associated parameters are given in table 1.

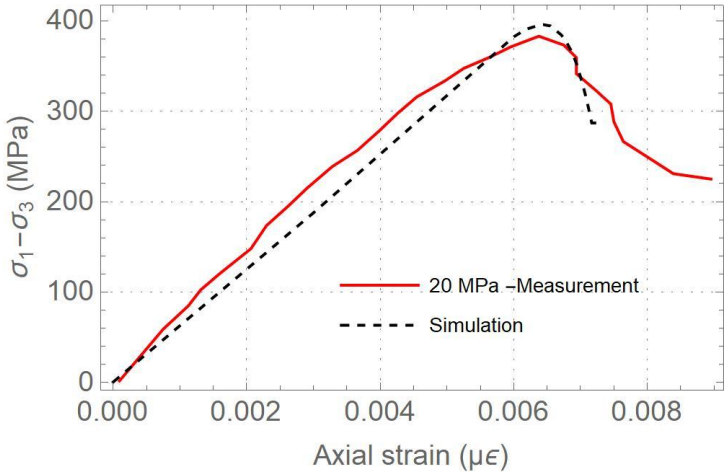


Figure 2. Mechanical calibration.

The originality of this work lies in the integration of the drilling fluid in contact with the rock to consider the continuous progression of the cooling front during rock cutting. This was made possible thanks to the Coupled Eulerian Lagrangian (CEL) method. The fluid phase in the CEL domain is modeled with an US–UP equation of state (EOS) rather than a constitutive relation (equation 1). For many fluids (e.g., water, air, drilling mud), the US–UP (Hugoniot) form provides a robust representation of shock-compression behavior:

$$U_s = c_0 + s \cdot U_p \tag{4}$$

where U_s is the shock velocity, U_p is the particle velocity, c_0 is the bulk (zero-pressure) sound speed, and s is the linear Hugoniot slope coefficient (Benson, 2004). In this formulation, the pressure in each Eulerian cell is obtained from the compressibility and internal energy through the Mie–Grüneisen-type extension of the Hugoniot, ensuring mechanically consistent computation of the thermodynamic state of the fluid. Because the fluid is initialized with uniform density, internal energy, and temperature, and because no spatially varying forcing terms (the drilling fluid is circulating and its temperature in contact with rock can be supposed constant) are introduced, the solution naturally evolves toward a spatially uniform pressure and temperature field.

Both air and water were considered by this method using the proper thermodynamic parameters gathered in table 2. The thermal exchange at the fluid-rock interface is governed by the classical heat exchange term:

$$\dot{q}_{ext} = -(A_s/m_f) \cdot h \cdot (T_f - T_s) \tag{5}$$

Where A_s is the wetted interface area between the fluid element and the solid surface, m_f is the mass of fluid contained in the Eulerian element, h is the convective heat-transfer coefficient in W/(m^2·K), T_f is the temperature of the fluid and T_s is the temperature of the solid surface in contact with the fluid. The main objective of considering fluids in this model using Eulerian formulation in contact with rock elements (Lagrangian) is to consider the actual value of pressure and temperature at the surface of the newly cut rock. This cannot be achieved by simply applying a constant temperature and pressure to the rock surface as a boundary condition.

Table 1. Rock properties.

Description	Values	Units
Elastic modulus	40	MPa
Mass density ρ	2000	kg/m^3
Thermal conductivity k	2.0	W/(m·K)
Heat capacity c_p	690	J/(kg·K)
Thermal expansion α_T	1e-5	1/K
C	50	MPa

φ_0,ψ_0	30°, 40°	
UCS	180	MPa
ε_0^P	0.0004	
dilatancy damage (β)	0.2	

Table 2. Fluid properties.

	Air	Water (liq.)	Units
Mass density ρ	1.225	1000	kg/m^3
Thermal conductivity k	0.025	0.6	W/(m·K)
Heat capacity c_p	1005	4180	J/(kg·K)
Dynamic viscosity μ	1.81·10^{-5}	0.001	Pa·s
US-UP EOS parameters (c_0, s, γ)	343, 1.0, 1.4	1500, 0.0, 0.1	Wave speed c_0 [m/s], linear Hugoniot slope s [-], Grüneisen γ [-]

2.3 Thermal Front Propagation

To compare the presented numerical response for a convective heat transfer case with an analytical solution in this section we consider the rock as a semi-infinite solid with a Dirichlet boundary conditions (constant temperature of the wellbore wall). The fluid is at a stable temperature and acts as a perfect heat-sink. The analytical heat transfer solution that describes the penetration of the thermal front inside the rock is given by (Bergman et al, 2011):

$$\frac{T(x,t)-T_w}{T_i-T_w} = \operatorname{erf}\left(\frac{x}{2\sqrt{\alpha t}}\right) \tag{6}$$

where α is the thermal diffusivity of the rock and t is the time. T_i is the initial temperature of the rock and T_w is the temperature at the wall (in contact with the perfect fluid) and x is the distance. This equation is compared to probed temperature values at certain depths inside the rock in Abaqus. The comparison can be seen in figure 3.

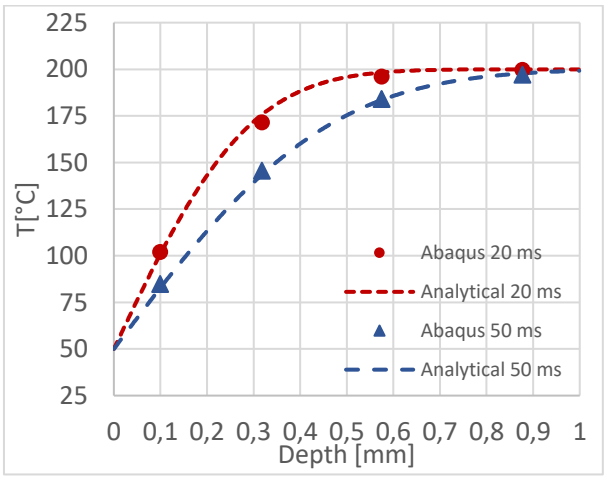


Figure 3. Thermal front propagation into the granite after 20 ms and 50 ms respectively.

The temperature of the fluid is 50 °C and the fluid of the rock is 200 °C. As can be seen in figure 3 the analytical equation and the numerical results from Abaqus show quite good agreement.

3 SINGLE CUTTER MODEL SET UP

The Finite Element Analysis (FEA) software Abaqus is used in this analysis where the PDC cutter is modeled as a rigid body. A CEL method is used for the interaction of the water with the rock. The fluid is a perfect Eulerian domain and the granite is modeled as a Lagrangian domain where the elements are deleted from the simulation at 90% deformation. Figure 4 shows a typical simulation result based on the experimental set up. It can be observed that freshly cut rock undergoes a cooling process immediately following the passage of the PDC cutter.

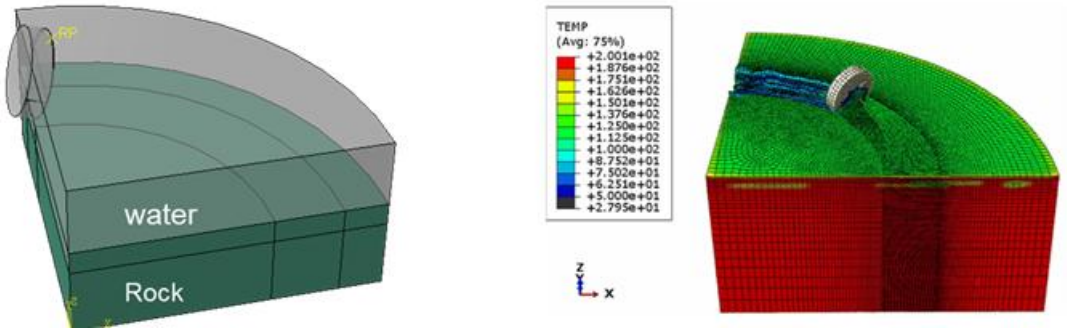


Figure 4. The cutter sweeping a path through the rock sample. The fluid domain (LHS) is made invisible in this case (RHS) to improve visuals. The temperature of the bulk of the rock is 200 °C and the temperature of the fluid is 50 °C.

4 RESULTS AND DISCUSSION

Figure 5 illustrates the comparative analysis between numerical simulations and experimental outcomes following eight rotations of the cutter and a penetration depth of 7 mm over a duration of 4.2 seconds. The general morphology of the simulated rock post-cutting is deemed satisfactory, and the simulated force values show good agreement with the measured forces, as depicted in Figures 6 and 7 for normal (Fn) and tangential (Ft) forces, respectively.

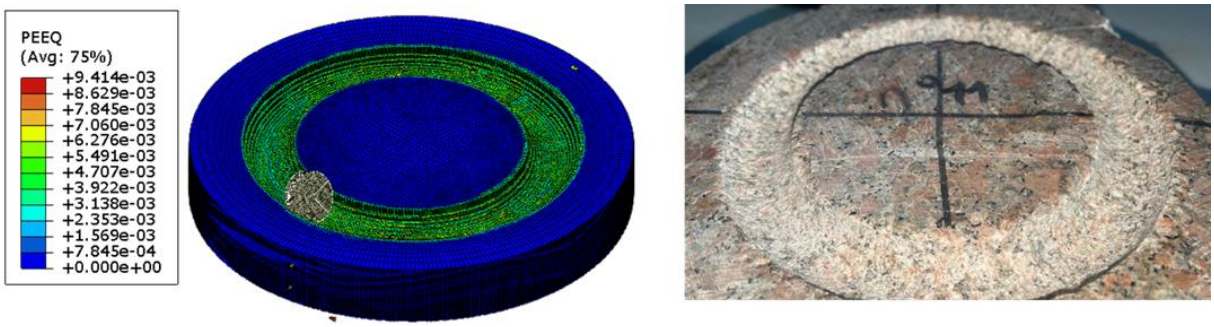


Figure 5. Numerical versus experimental results after 8 rotations. In Abaqus, PEEQ stands for equivalent plastic strain.

Figures 6 and 7 show the cutting forces under ambient temperature, air cooling and water-cooling conditions. It should be noted that a 100 Hz filter was applied to numerical results to obtain smoother and comparable curves. It can be observed that both normal and tangential forces decrease with cooling phases with a more pronounced effect observed in the case of water cooling. Under ambient temperature conditions the initial Fn/Ft ratio is 0.8, and approaches unity when water cooling is applied. This observation underscores the efficacy of fluid cooling in significantly diminishing the tangential cutting forces, which is indicative of a reduction in rock shear strength facilitated by water cooling as opposed to air cooling techniques. The numerical results are globally in good agreement with the experimental ones where the predicted Ft values are slightly higher than those measured. This effect is associated with the homogenous rock model assumption wherein the differential thermal expansion coefficients of the various constituents of granite are represented by a singular mean value. This approach neglects the differential thermal stresses that can further weaken the mechanical properties of the rock. Heterogenous rock, rather than homogenous rock, would have to be modeled in order to include this phenomenon.

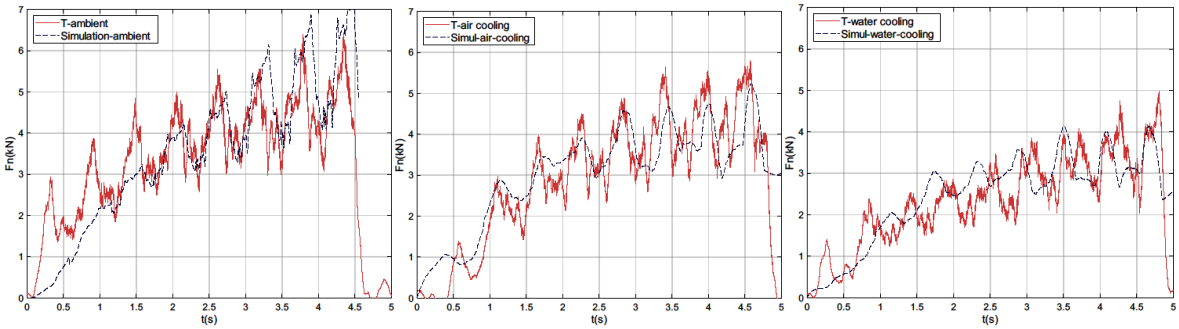


Figure 6. Numerical (dashed line) and experimental results (red). From left to right: Normal cutting force for respectively under ambient temperature, air cooling and water cooling.

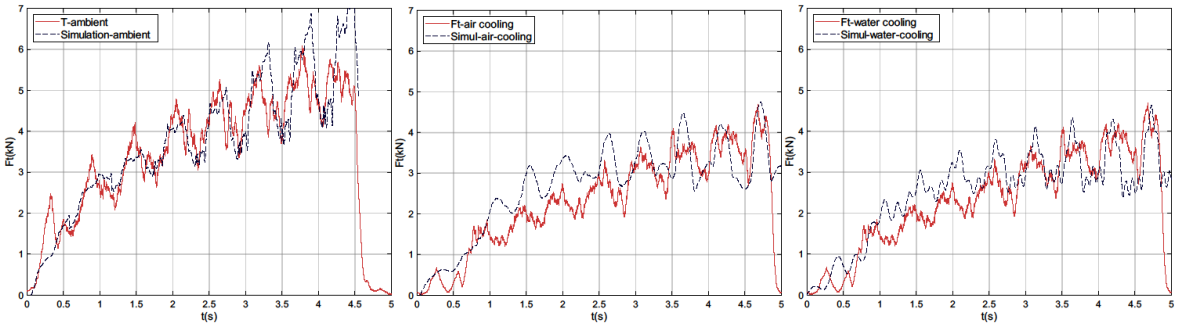


Figure 7. Numerical (dashed line) and experimental results (red). From left to right: Tangential cutting force for respectively under ambient temperature, air cooling and water cooling.

4.1 Sensitivity analysis

A convenient metric to compare the effort it takes to remove a certain volume of rock is the mechanical specific energy (MSE) often expressed in J/mm^3 or in MPa.

$$MSE = \frac{1}{V}\int F \cdot dl \tag{7}$$

where F is the force, $\int F \cdot dl$ is the integral of this force over the cutting path and V is the volume of removed rock. The jagged force can have many fluctuations as the rock chipping is a discrete process. The force time trace will be noisy in both experiments as well as FEA. By use of the MSE a smoother trend can be achieved, independent of number of turns.

In the following figures, the simulation results are presented in terms of Mechanical Specific Energy (MSE, in MPa or normalized) for different rates of penetration (ROP, meters per hour), angular velocities (RPM, rotations per minute) and temperature difference (ΔT, degrees Celsius). Given the extensive computational demands of the complete simulation process, for the purposes of sensitivity analysis, we conducted simulations on only one-quarter of the model, as depicted in Figure 4. It is important to note that achieving the validation cases (illustrated in Figures 6 and 7) necessitated more than 900 hours of computation (CPU time) on a 24-core Intel i7 computer system.

Figure 8 shows the MSE evolution for two different ROPs (10 m/h and 20 m/h) while RPM and temperature evolve. The findings indicate that there exists an optimal range for the ROP and RPM in relation to the progression of the thermal front and the thermal diffusion process. When either of these parameters exceed the thermal cooling front, the improvement in MSE reduction becomes negligible. Conversely, operating within the cooled zone at an ROP of 10 meters per hour, coupled with a reduced RPM, results in a significant and advantageous reduction in MSE values.

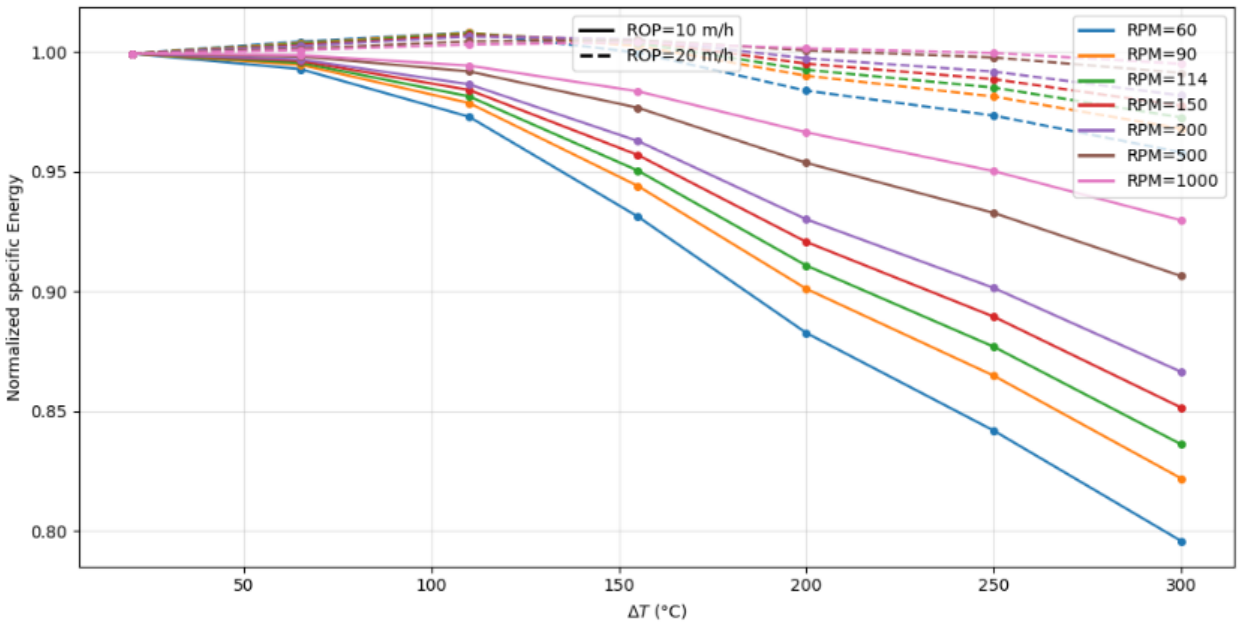


Figure 8. Normalized MSE evolution according to drilling parameters and different temperatures (water cooling was considered).

Figure 9 illustrates the impact of DOC on the MSE value across three distinct temperature differentials (ΔT). The advantageous effect of cooling spans a range from 50%, observed at a DOC of 0.5 mm and ΔT of 200 °C, to 1%, recorded at a DOC of 2 mm and ΔT of 100 °C.

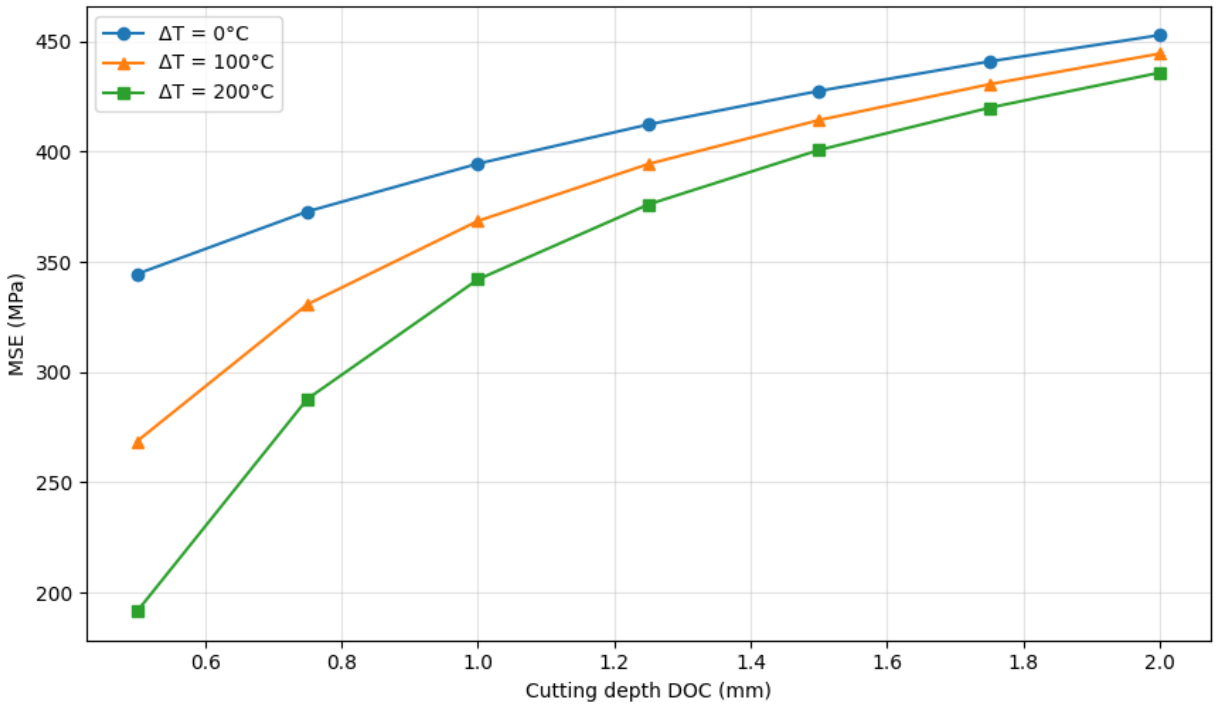


Figure 9.MSE evolution for different DOC and ΔT.

5 CONCLUSION

A laboratory scale single cutter test under two cooling conditions was developed and tested on Red Bohus granite. Subsequently, numerical modelling was developed to simulate the laboratory test under dynamic conditions using Abaqus software.

The results clearly demonstrate that the normalized MSE decreases with increasing thermal gradient (ΔT), confirming the beneficial effect of rapid rock cooling on drilling efficiency. At higher rotation rates (≥ 500 RPM),

the reduction in normalized MSE becomes less sensitive to ΔT, suggesting that dynamic effects and limited cooled depth partially counteract the thermal weakening. Conversely, for moderate RPMs typical of field operations (90–150 RPM), cooling of 200 °C leads to an MSE reduction of up to 20%, signifying substantial energy savings and enhanced drilling performance. This ratio could be further enhanced by considering rock heterogeneity, where differential thermal expansion of each rock component could further weaken the rock and, consequently, reduce the global MSE value.

Overall, these results validate that shock cooling of the rock surface in a controlled environment significantly decreases drilling energy demand by thermally weakening the bit-rock interaction surface structure of the granitic formation. This highlights the potential of thermo-mechanical strategies to optimize drilling performance and extend bit life in deep granitic formations, where conventional purely mechanical drilling is energy intensive.

However, the rapid cooling effect at the highest thermal difference between the drilling fluid and rock surface must be analyzed in reference to the wellbore stability of previously drilled sections, where it might negatively cause drilling issues in deep and hot wells. This could be a topic for future study.

The practical application of this work can be considered in designing fit-for-purpose drilling systems, where the highest thermal difference is achieved between the drilling fluid and granitic formation at the bit-rock interface surface. This can be achieved with insulated drill pipe, heat-absorbing drilling fluids, surface mud cooling facilities, and other existing heat management solutions. Correspondingly, drilling parameters may be controlled in favor of longer drill bit life, with lower angular velocities (RPM), and controlled depth of cut (DOC) via applied weight on bit (WOB) to smoothen the bit-rock interaction and extend life of the PDC bit. Existing autonomous drilling control tools allow for precise management of drilling parameters in real-time, with downhole and surface sensors processing data, adjusting the DOC automatically at the sub-second cadence. When such a system is applied in the deep geothermal drilling process of the crystalline basement, it may lead to much longer sections of the wellbore drilled in a single run before tripping out of hole to replace the worn-out drill bit. This could lead to cost savings in geothermal well construction, therefore reducing the price per geothermal energy unit for end users.

REFERENCES

Saksala T.: Numerical modelling of thermal jet assisted rock cutting with double PDC cutters, International Journal for Numerical and Analytical Methods in Geomechanics, 48-10, (2024), 2700-2723.

Zhang Z. and Zhao D.: 3D numerical simulation study of rock breaking of the wavy PDC cutter and field verification, Journal of Petroleum Science and Engineering, 203, (2021).

Dai Z. and Hu J.: Reconstruction of 3D Shapes of Granite Minerals and Generation of Random Numerical Specimens, GeoScienceWorld, 1422262, (2022), 17 pages.

Liu W. and Deng H.: The rock cutting simulation of heterogeneous granite using FDEM method, Petroleum, 11-1, (2025), 1-12.

Weiji Liu, Xudong Qian, Tao Li, Yunlai Zhou, Xiaohua Zhu, Investigation of the tool-rock interaction using Drucker-Prager failure criterion, Journal of Petroleum Science and Engineering, Volume 173, 2019, Pages 269-278, ISSN 0920-4105.

Bergman et al.: Fundamentals of Heat and Mass Transfer, John Wiley & Sons, 7, (2011), 2631 pages.

Shen Y., Yuan J., Hou W., Hao J., Bai Z., Li T. The strength changes and failure modes of high-temperature granite subjected to cooling shocks, Geomechanics and Geophysics for Geo-Energy and Geo-Resources, 7-1, (2021), 23.

Jahangir E., Gerbaud L., Goelema B., Rogers A., and Vetsak A. Numerical and Experimental investigation on cooling-assisted rock drilling. Submitted to International Journal of Rock mechanics and Rock Engineering, (October 2025).

Ma Q., Liu X., Wang E., Xu Q., Wang C., Yao W., and Nan Hu. Micromechanical behavior of granite under high temperature with enhanced mori-tanaka model, Journal of Rock Mechanics and Geotechnical Engineering, (2025), ISSN 1674-7755.

Xiao P., Zheng J., Dou B., Tian H., Cui G., and Kashif M. Mechanical Behaviors of Granite after Thermal Shock with Different Cooling Rates, Energies, 14(13), (2021), 3721.

Wu X., Huang Z., Song H., Zhang S., Cheng Z., Li R., Wen H., Huang P. and Dai X. Variations of Physical and Mechanical Properties of Heated Granite After Rapid Cooling with Liquid Nitrogen, Rock Mechanics and Rock Engineering. 52, (2019), Pages 2123-2139.

Benson, D. J., "Contact in a Multi-Material Eulerian Finite Element Formulation," Computer Methods in Applied Mechanics and Engineering, vol. 193, (2004). pp. 4277–4298.

Khodayar M. and Bjornsson S. Conventional geothermal systems and unconventional geothermal developments: An overview. Open Journal of Geology, 14:196–246, (2024).

Dassault Systèmes. (2024). *Abaqus 2024 Documentation*. Providence, RI, USA: Dassault Systèmes Simulia Corp.